

On the Fission of Elementary Particles and the Evidence for Fractional Electrons in Liquid Helium

H. J. Maris*

*Department of Physics, Brown University, Providence, Rhode Island 02912, USA
and*

*Laboratoire de Physique Statistique, Ecole Normale Supérieure,
24 Rue Lhomond, 75231 Paris 05, France*

(Received March 2, 2000; revised April 6, 2000)

We consider the possibility that as a result of interactions between an elementary particle and a suitably designed classical system, the particle may be divided into two or more pieces that act as though they are fractions of the original particle. We work out in detail the mechanics of this process for an electron interacting with liquid helium. It is known that when an electron is injected into liquid helium, the lowest energy configuration is with the electron localized in a $1s$ state inside a spherical cavity from which helium atoms are excluded. These electron bubbles have been studied in many experiments. We show that if the electron is optically excited from the $1s$ to the $1p$ state, the bubble wall will be set into motion, and that the inertia of the liquid surrounding the bubble can be sufficient to lead to the break-up of the bubble into two pieces. We call the electron fragments "electrinos." We then show that there is a substantial amount of experimental data in the published literature that gives support to these theoretical ideas. The electrino bubble theory provides a natural explanation for the photoconductivity experiments of Northby, Zipfel, Sanders, Grimes and Adams, and possibly also the ionic mobility measurements of Ihas, Sanders, Eden and McClintock. Previously, these experimental results have not had a satisfactory explanation. In a final section, we describe some further experiments that could test our theory and consider the broader implications of these results on fractional particles.

I. INTRODUCTION

Quantum mechanics has been the accepted fundamental theory of physics for the last 70 years. The energy levels of atoms that are obtained through solution of the time-independent Schrödinger equation are in very accurate agreement with an enormous range of experimental data. Quantum mechanics has also been used to calculate scattering cross sections, again

* E-mail: humphrey_maris@brown.edu.

leading to agreement with experiment. However, almost from the time that the principles of quantum mechanics were formulated, there has been controversy about the measurement process. For example, Einstein, Podolsky, and Rosen¹ have claimed that quantum mechanics, taken together with the standard view of the quantum measurement process, leads to results that indicate that quantum mechanics does not provide a complete description of physical reality. Their argument was rejected by Bohr,² who argued that the procedure of measurement itself is implicitly part of the definition of physical quantities. While such questions are interesting, it appears more important to establish, as an essential element of quantum theory, some number of principles that in conjunction with the equation for the time-development of the wave function make the theory complete in the sense that there is a clear and definite prediction for the result of any experiment that can be performed. These principles can be selected only on the basis of a comparison of theory and experiment.

The difficulties in quantum theory arise largely at points where the classical and quantum worlds meet.³ The traditional view has been that a quantum mechanical experiment involves elements that are essentially non-quantum. A classical apparatus under the control of a human brain prepares the quantum system in some way. The measurement of the outcome of an experiment is considered to be some numbers that are ultimately read from a classical instrument.

In this paper we shall consider a particular experimental situation that is designed to bring into a very sharp focus some of the uncertainties of quantum measurement theory. This investigation leads, in turn, to some remarkable results concerning the fission of the electron, and by implication the fission of other elementary particles.

II. COMMENTS ON THE FISSION OF ELEMENTARY PARTICLES

One type of fission of an elementary particle takes place when a wave packet is incident on a potential barrier. A part of the wave packet is transmitted, and a part is reflected. At some later time, measurements are made to determine the location of the particle. According to the conventional interpretation of quantum theory, the probability that the particle will be found on the right hand side of the barrier is

$$P_{\text{R}} = \int_{\text{RHS}} |\psi|^2 dV, \quad (1)$$

where the integral is over all of space on the right hand side of the barrier. If the particle is found on the right, the wave function everywhere on the

left hand side is supposed to immediately become zero; this is referred to as collapse of the wave function. This collapse ensures that if a second measurement of P_R is made a short time later, the particle will again be found on the right.

Consider now a different experiment. A particle is confined to a box that has a movable impenetrable partition (Fig. 1a). Let ψ_L and ψ_R be the lowest energy solutions of Schrödinger's equation for the left and the right hand parts of the box when the partition is in the closed position, and let the energies corresponding to these solutions be E_L and E_R , respectively. Suppose that we start with the partition in the open position and the particle in the ground state. If the partition is then closed very slowly, it follows from the adiabatic principle that the particle will remain in the ground state. Thus, if $E_L < E_R$ the wave function will be completely confined to the left hand part of the box. Then, $P_L = 1$ and $P_R = 0$. Now suppose that the partition is closed rapidly. In this case, the system will not remain in the ground state, and the wave function will be non-zero in both the left and right regions. If a measurement of P_R is made, quantum theory predicts that the result is as given by Eq. (1). If the particle is found on the right, the wave function on the left becomes zero immediately, even though

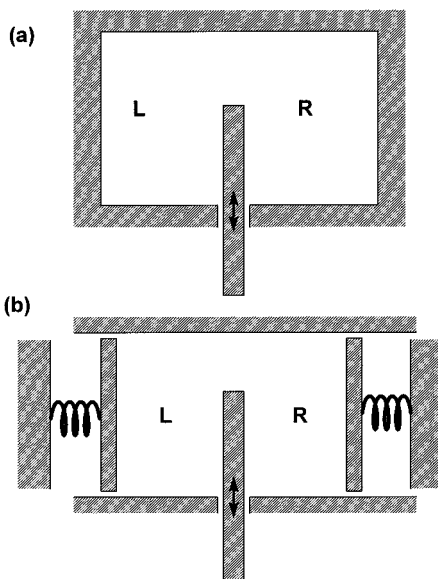


Fig. 1. (a) Box with a movable partition to divide the wave function into two parts. (b) Box with movable partition and end walls with springs.

the barrier is completely impenetrable to the particle. To perform an experiment of this type appears to be feasible in principle, but we are not aware of a specific example.

Now consider a variation of this experiment. Let us suppose that the end walls of the box are not rigid, but instead are held in place by springs as shown in Fig. 1b. The particle will exert a pressure P on the left hand end wall given by

$$P = \frac{\hbar^2}{2m} |\nabla\psi|^2, \quad (2)$$

where $\nabla\psi$ is the gradient of the wave function at the wall, and m is the mass of the particle. The force on the end wall is thus dependent on the wave function. The wave function is a function of the size and shape of the box, and so is, in turn, dependent on the position of the end wall. If there is some mechanism that damps the motion of the end wall, the wall will come to rest at a position that minimizes the sum of the energy of the spring and the energy of the particle. Suppose now that the position of the end wall is measured in some way. If it is found that the spring is compressed relative to its natural length, the wave function inside the box must be non-zero. For a given spatial dependence of the wave function, the probability of finding the particle inside the left part of the box is directly proportional to the wall displacement.

One can ask a number of questions about the results of experiments on this system:

(1) Is the discussion just given in accord with experiment? In other words, if such a mechanical system is constructed, and if a partition is moved across the box in a way such that one would expect based upon the time-dependent Schrödinger equation that ψ should be non-zero on both sides of the partition, will there be a displacement of the end wall that can be calculated from the pressure as given by Eq. (2)?

(2) If the position of the left hand wall is measured, and it is found that the wall is displaced, what is the effect of this measurement on subsequent measurements of the displacement of the right hand wall? For example, does the determination that there is *some* displacement of the left hand wall result in a sudden change in the wave function such that ψ becomes zero on the right hand side? This would presumably mean that a second measurement of the displacement of the left hand wall would give a different, and larger, displacement because now the wave function is entirely on the left.

(3) If the left hand part of the box is illuminated with light, at what frequencies will optical absorption take place?

III. ELECTRONS IN LIQUID HELIUM

One can imagine a number of ways of performing an experiment related to those just described. We now describe in some detail one particular experimental situation. This concerns the states of an electron that has been injected into liquid helium. Electrons in helium have been studied in many experiments over the last 30 years.⁴ An electron is attracted to a helium atom at large distances, but is repelled at short distances because of the Pauli principle. As a result, a low energy electron entering liquid ⁴He has to overcome a potential barrier V_0 of approximately 1 eV.⁵ Because the interatomic forces in helium are so weak, an electron injected into helium forms a structure referred to as an electron bubble. The electron sits in a cavity in the liquid from which essentially all helium atoms are excluded. As a first approximation, the energy of this bubble can be taken to be the sum of the energy E_{el} of the electron, the surface energy of the bubble, and the energy of creating the bubble volume. Thus,

$$E = E_{el} + \alpha \int dA + P \int dV, \quad (3)$$

where α is the surface energy of helium per unit area, P is the applied pressure, and the integrals are over the surface and volume of the bubble. If the penetration of the electron wave function into the helium is neglected, and we consider an electron in the 1s state, Eq. (3) becomes

$$E = \frac{h^2}{8mR^2} + 4\pi R^2\alpha + \frac{4}{3}\pi R^3P, \quad (4)$$

where m is the mass of the electron, and R is the radius of the bubble. If the pressure is zero, the lowest energy is obtained with a radius of

$$R_0 = \left(\frac{h^2}{32\pi m\alpha} \right)^{1/4}. \quad (5)$$

This is the radius of a spherical bubble containing an electron in the ground state. One can also find the equilibrium shape and size of a bubble containing an electron in an excited state (see Sec. IIIB below).

There are a number of corrections that can be considered.

(1) The radius R_0 of the electron bubble calculated from Eq. (5) for $T=0$ K, and with zero applied pressure, is 19.4 Å. The width of the liquid-vapor interface is 7 Å,⁶ and thus is not entirely negligible compared to the bubble radius. It is possible to use a density functional method to make an approximate correction for the finite thickness of the bubble wall.⁷

(2) The electric field due to the electron causes a polarization of the helium atoms surrounding the bubble. The interaction of this polarization with the electric field gradient gives an inward force on the helium, and the bubble radius is reduced.⁸

(3) At finite temperatures the electron bubble will contain some helium vapor. The effect of vapor inside the bubble becomes important at temperatures above about 3 K.⁷

(4) Since the height V_0 of the barrier is finite, there will be some penetration of the electron into the helium. This penetration lowers the energy of the electron by a small amount. The barrier height is expected to depend on pressure.⁴

(5) The surface energy of the liquid should depend on the pressure.⁹ This variation has not been measured experimentally. It is also possible that the surface tension is modified by the proximity of the electron to the surface.

(6) Finally, since the radius of the bubble is not much larger than the interatomic spacing, it may be necessary to include in the calculation a correction to allow for the curvature of the liquid surface.

In this paper we are primarily interested in temperatures below 1.5 K, so the effect (3) of helium vapor is unimportant. Of the other effects, it has been shown that the corrections (1) and (2) to the energy arising from the finite width of the liquid-vapor interface and from the polarization of the helium are small.⁷ Effects (5) and (6) can, in principle, be included through the use of a density functional scheme that correctly represents the energy of helium with a non-uniform density. We have used this method in a previous paper to calculate the configuration of a bubble with the electron in the ground state.⁷ However, it appears to be very difficult to extend this calculation to determine the properties of a bubble in which the electron is in an excited state. Consequently, we will use a simplified approach due to Grimes and Adams,¹⁰ together with some further simplifications that are needed to make some of the calculations tractable. Grimes and Adams showed that the experimentally-measured photon energies E_{1s-1p} and E_{1s-2p} for transitions from the ground 1s state to the 1p and 2p states,

respectively, were in good agreement with results calculated for a simplified model. They took the surface energy α to have a constant value of $0.341 \text{ erg cm}^{-2}$, independent of pressure, and used the Wigner-Seitz approximation to estimate the pressure dependence of V_0 . The polarization energy (2) was included.⁸ Effect (3) was neglected because of the low density of helium vapor at. Effects (1), (5) and (6) were also neglected.

We make two further simplifications of the model of Grimes and Adams. In all of the calculations, we will neglect the polarization energy. This makes a small contribution to the total energy of the bubble, and is difficult to treat correctly for bubbles with electrons in excited states.⁸ We show in the next section that when this contribution to the energy is neglected, the Grimes/Adams model still gives very good agreement with the experimental data for E_{1s-1p} and E_{1s-2p} . In addition, in some of the calculations, we will neglect the effect of the penetration of the wave function into the helium. This approximation is also introduced to make the calculations easier for bubbles with electrons in excited states.

A. Calculation of Energies for Optical Absorption

The energy E_{1s} of a bubble in which the electron is in the 1s state is shown as a function of pressure in Fig. 2. Note that the total energy of the bubble is plotted, including the surface and volume terms. For each pressure the bubble has an equilibrium radius $R_{1s}(P)$ that minimizes the

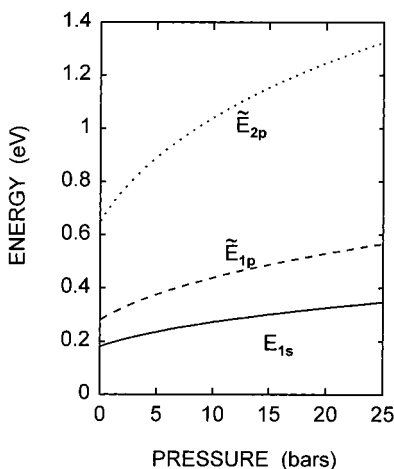


Fig. 2. Energy of the 1s, 1p and 2p states as a function of pressure. For all of these states the radius of the bulb is equal to the equilibrium radius of the 1s bubble.

total energy. Also included in this figure are the energies \tilde{E}_{1p} and \tilde{E}_{2p} of spherical bubbles of the same radius, but with the electron in the higher energy states 1p and 2p, respectively. The tilde is to denote that these energies do not correspond to states in which the bubble is in mechanical equilibrium, i.e., the size and shape of the bubble has not been adjusted to minimize the total energy. The energies shown in Fig. 2 are calculated for an electron moving in a spherical bubble with a potential V_0 outside the bubble, i.e., in these calculations allowance is made for the penetration of the wave function into the helium. The radius for the 1s bubble at zero pressure is found to be 17.9 Å, only slightly less than is found when the penetration of the wave function into the helium is neglected.

According to the Franck–Condon principle, when the electron is in the ground state, optical absorption can occur at the photon energies $E_{1s \rightarrow 1p} = \tilde{E}_{1p} - E_{1s}$, and $E_{1s \rightarrow 2p} = \tilde{E}_{2p} - E_{1s}$. These photon energies are plotted in Fig. 3. Also included in Fig. 3 are the data of Grimes and Adams^{10, 11} for the 1s → 1p, and Zipfel and Sanders for the 1s → 2p transition.^{12, 13} It can be seen that the agreement between the calculation and the data is very good.

B. Calculation of Equilibrium Shapes for Excited States

To calculate the equilibrium shape of a bubble containing an electron in an excited state, the following steps are necessary. A shape for the

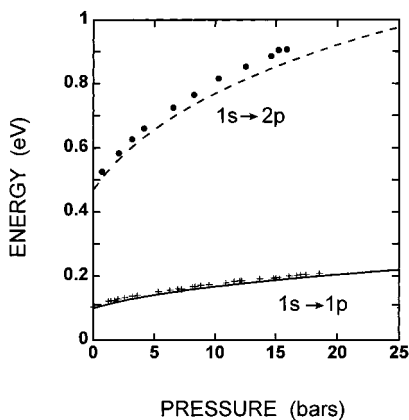


Fig. 3. Energy of the 1s → 1p and 1s → 2p transitions as a function of pressure. Solid curves show the results of the calculation described in the text. The crosses are the data points of Grimes and Adams, Ref. 10, and the circles the data of Zipfel, Ref. 12.

helium bubble is assumed. The Schrödinger equation for the electron is then solved with a potential energy that is zero inside the bubble and V_0 outside. For a given set of quantum numbers for the electron state, the shape of the bubble is then varied so as to minimize the total energy. The total energy E is given by Eq. (3). The shape and total energy of bubbles containing an electron in an excited state have been calculated previously by Duvall and Celli.¹⁴ They used a perturbation approach in which the distortion of the shape from spherical was treated as a small parameter. The energy of some of these states has also been estimated by Fowler and Dexter,¹⁵ who used a simplified model in which the bubble shape was taken to be a rectangular box.

In this paper, we will consider only bubble shapes that have axial symmetry. Thus the wave function of the electron inside the bubble will have a definite azimuthal quantum number m , and can be written as

$$\psi(r, \theta, \phi) = \sum_l A_l P_l^m(\cos \theta) e^{im\phi} j_l(kr), \quad (6)$$

where A_l are coefficients to be determined, $P_l^m(\cos \theta)$ are associated Legendre polynomials, $j_l(kr)$ is a spherical Bessel function, and $k = (2mE_{\text{el}})^{1/2}/\hbar$. As a first step, we calculate the electron energy in the limit $V_0 \rightarrow \infty$, so that ψ is zero at the bubble wall. An initial guess is made for the energy E_{el} . The sum over l extends up to some maximum value l_{max} . To look for a state of even parity, the coefficient A_0 is set equal to unity, and all of the $\{A_l\}$ for odd l are set equal to zero. Then the remaining coefficients are adjusted so as to minimize the integral

$$S \equiv \iint |\psi(r, \theta, \phi)|^2 d \cos \theta d\phi. \quad (7)$$

This integral is over the surface of the bubble. This minimization procedure leads to a set of linear equations for the $\{A_l\}$ coefficients. Let the value of S after the $\{A_l\}$ have been chosen in this way be S_{min} . Then the energy E_{el} is adjusted to find values at which S_{min} becomes close to zero. Since for these energies Schrödinger's equation is satisfied inside the bubble and also ψ is very small on the surface of the bubble, these values of E_{el} must be the energy eigenvalues. The eigenfunction can then be calculated from the $\{A_l\}$ coefficients. To find states of odd parity the same procedure is used except all the even l coefficients are set zero, and $\{A_1\}$ is set equal to unity. If l_{max} is chosen to sufficiently large, the results for E_{el} are independent of l_{max} .

For each excited state there will be a shape of the electron bubble that corresponds to a minimum energy. We refer to this as the equilibrium

shape. To find this shape we have to look for a minimum in the total energy as described above. To find the shape that minimizes the energy, we write

$$\tilde{R}(\theta) = \sum a_L P_L(\cos \theta), \quad (8)$$

where $\tilde{R}(\theta)$ is the distance from the origin to the bubble surface in the direction θ , $P_L(\cos \theta)$ are Legendre polynomials, and $\{a_L\}$ are some coefficients. The summation is over even values of L from zero to a maximum value L_{\max} . Note that only shapes with axial symmetry are considered. The set of $\{a_L\}$ coefficients are then varied to obtain the minimum energy. The equilibrium shapes of several excited states for zero pressure are shown in Fig. 4. These results were obtained with $L_{\max} = 6$; the use of a larger value does not change the shapes significantly.

The eigenvalues obtained in this way do not allow for the penetration of the wave function into the barrier. Given the uncertainties in the model, this appears to be a reasonable approximation. As a test, we have calculated the energies \tilde{E}_{1s-1p} and \tilde{E}_{1s-2p} for $P=0$ when ψ is required to go to zero at the bubble wall, and also when the wave function penetrates into the helium. We find that when there is no penetration, \tilde{E}_{1s-1p} and \tilde{E}_{1s-2p} are increased by only 5 and 7%, respectively, compared to the values found for these quantities when penetration is taken into account.

The bubble shapes can be understood qualitatively in terms of the balance between the pressure exerted on the bubble wall by the electron, the surface tension, and by the liquid pressure. The pressure exerted by the

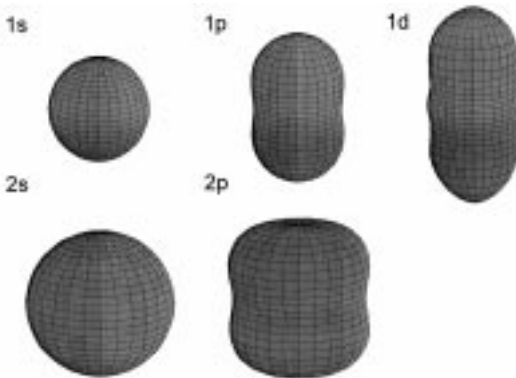


Fig. 4. The shape of bubbles containing electrons in different quantum states. The liquid pressure is zero. The same scale is used for each state, and the radius of the 1s bubble is 19.4 Å.

electron is given by Eq. (2). For the 1p state, for example, the electron pressure vanishes in the plane $z = 0$, and the bubble has a slight waist coinciding with the xy -plane. As the pressure is increased, the size of the bubble decreases, and the waist becomes more pronounced. As an example of this, we show in Fig. 5 the shape of the bubble with the electron in the 1p state at pressures of 0, 5 and 10 bars. At pressures of 10 bars and above, the waist of the bubble has a radius of only a few Angstroms. It can be seen from Fig. 5 that at high pressure the bubble shape is closely approximated by two spheres of equal radius R_2 that overlap by a small amount. The wave function inside each sphere is a 1s wave function with origin at the center of the sphere. The wave functions in the two spheres have opposite signs. We can consider that each sphere has an energy of

$$E_{1/2} = \frac{1}{2} \frac{h^2}{8mR_2^2} + 4\pi R_2^2 \alpha + \frac{4}{3} \pi R_2^3 P. \quad (9)$$

This formula is identical to the expression for the energy of a bubble containing a 1s state electron [Eq. (4)], apart from the factor of $\frac{1}{2}$ that arises because each of the spheres contains only one half of the electron wave function. In this pressure range, where the waist radius is small, the numerical method that we are using to solve Schrödinger's equation becomes inaccurate unless a very large value of l_{\max} is used. We have confirmed that the energy E found by numerical solution is close to the value $2E_{1/2}$.

Although it would be interesting to have more detailed information about the precise shape of the equilibrium 1p state at high pressures, there seems to be little point in attempting a more accurate solution of Schrödinger's equation. The simplified model that we are using (see

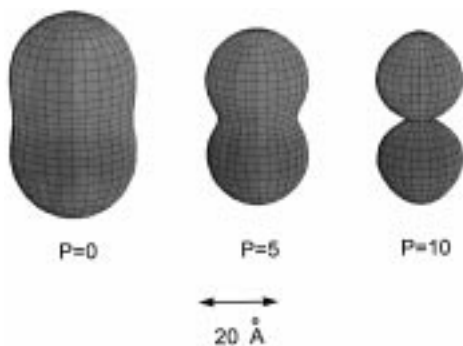


Fig. 5. The shape of the electron bubble containing a 1p state at pressures of 0, 10, and 20 bars.

discussion at beginning of this section) cannot be used to consider what happens when the radius of the waist approaches atomic dimensions. To make a quantitative study of the shape it would be necessary to construct a more elaborate model, perhaps based on some form of density functional model for the helium. Nevertheless, the calculation that we have done clearly shows that at high pressures the $1p$ bubble is greatly distorted, and is close to being pinched off into two separate volumes. At 10 bars, for example, the energy E_{1p} that we have computed by solving Schrödinger's equation numerically and then adjusting the shape of the bubble so as to minimize the total energy, is very close to twice the energy $E_{1/2}$ that is obtained from Eq. (9).

Note that we have considered the equilibrium shapes of the states with $m = 0$ only.

C. Dynamics of the Optical Absorption Process

The calculations in the previous section all concern the equilibrium shape of an electron bubble. We now consider what happens when an electron is optically excited from the ground state into one of the higher states, such as the $1p$. The time scale for electron motion is of the order of mR^2/h , where R is the radius of the bubble. This time is of the order of 10^{-14} s. The time scale for the motion of the bubble wall is of the same order as the period for shape oscillations of the bubble; if the liquid pressure is zero, this period is of the order of $(\rho R^3/\alpha)^{1/2}$, and is in the range 10^{-10} to 10^{-11} s. Thus, the Franck–Condon principle applies, i.e., it should be considered that the transition of the electron occurs before the bubble has had time to change shape.¹⁶ A complete calculation of the motion of the bubble after optical excitation would require the following steps. The bubble starts as a sphere of the same radius as the equilibrium $1s$ state. For this bubble size, the $1p$ wave function is found. The net pressure at each point on the bubble wall due to the combined effects of the electron, the surface tension, and the liquid pressure can then be determined. This pressure varies over the surface of the bubble, and so the bubble surface begins to move. This results in a velocity field in the liquid. To determine how the shape of the bubble evolves, it is therefore necessary to calculate at each instant of time the electron wave function, the force on the bubble wall, and how this force changes the motion of the liquid. It should be a reasonable approximation to treat the liquid as an incompressible fluid. At low temperatures, e.g., at around 1.2 K or below, the effects of dissipation should be very small. We discuss this point in more detail below.

Although this calculation is straightforward in principle, it requires substantial numerical computation, and we have not attempted to perform

it. Instead, we have restricted attention to the examination of the potential energy surface in the configuration space of parameters defining the bubble shape. At the simplest non-trivial level, the shape of the bubble can be parameterized by just two coefficients a_0 and a_2 [see Eq. (8)]. The energy E from Eq. (3), which plays the role of the potential energy in the dynamical problem, can then be represented by a contour plot in the a_0 - a_2 plane (Fig. 6). The starting configuration immediately after excitation from the 1s to the 1p states corresponds to $a_0 = 19.4$, $a_2 = 0 \text{ \AA}$,¹⁷ and the energy is 4.828×10^{-14} ergs.¹⁸ The minimum energy is 4.275×10^{-14} ergs, and is at $a_0^{\min} = 21.0 \text{ \AA}$, and $a_2^{\min} = 8.8 \text{ \AA}$. After excitation the bubble will move on some path in the a_0 - a_2 plane. If the motion is heavily damped by the viscosity of the liquid, the bubble will change shape slowly and will eventually reach the configuration of minimum energy. However, if the damping is small, the bubble can explore the entire region of the a_0 - a_2 plane in which the energy is less than its starting energy. It can be seen from Fig. 6 that this region extends out to the line on which $a_2 = 2a_0$. On this line, the distance from the center of the bubble to the bubble surface

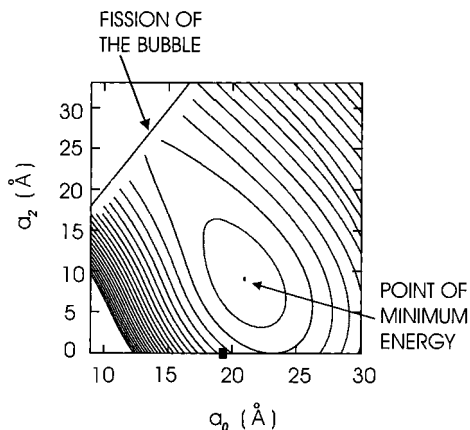


Fig. 6. Contour plot of the energy of a bubble containing a 1p electron as a function of the parameters a_0 and a_2 . The distance from the center of the bubble to the surface in the direction θ is $a_0 P_0(\cos \theta) + a_2 P_2(\cos \theta)$. The contour closest to the energy minimum at 4.275×10^{-13} ergs corresponds to an energy of 4.4×10^{-13} ergs, and the energy difference between adjacent contours is 0.2×10^{-13} erg. Along the line on which $a_2 = 2a_0$, the waist of the bubble has zero radius, and the bubble has split into two. The solid black square indicates the configuration of the bubble immediately after excitation to the 1p state.

is zero for $\theta=0$, i.e., the waist of the bubble becomes zero and the bubble breaks into two parts. It is hard to make an accurate calculation of the energy of the electron close to this line because it is necessary to use a large value for l_{\max} in Eq. (6). However, it appears that the lowest energy along the line on which fission occurs is significantly below the starting energy of 4.828×10^{-14} ergs. Therefore, in the absence of damping the bubble can reach the line and undergo fission.

We have not performed detailed calculations of the energy as a function of a_0 and a_2 at different pressures. However, it is clear that as the pressure is increased, the equilibrium state of the bubble moves closer to the fission line ($a_2 = 2a_0$), and that the amount by which the starting energy of the bubble in the 1p state exceeds the energy at the fission line will go up.

D. Stability of the Fission Process

In the previous section we have considered the possibility of fission resulting from a dynamical process after optical excitation. At first sight, this calculation can be objected to on stability grounds. It could be argued that as the bubble waist is about to pinch off and divide the bubble into two pieces, one of the pieces of the bubble will always be slightly larger than the other. The pressure inside a bubble due to surface tension is given by Laplace's formula $P = 2\alpha/R$, and so the pressure will always be larger in the smaller bubble. Hence, this bubble will shrink and the wave function will be driven into the larger bubble which will grow. Thus, all of the electron wave function will transfer into the larger bubble, the smaller bubble will collapse, and fission will not take place.

We now show that this argument is wrong. We are interested here in knowing what happens when the wave function of an electron in the 1p state is close to being divided into two pieces. The 1p state has a node in the region where the bubble waist will be pinched off. We consider as a highly-simplified model system a particle that moves in one dimension in a potential consisting of two wells each of width a (Fig. 7a). The wells are separated by a barrier of height U . For this model system, there is a state in which the wave function has an equal amplitude in each well, but opposite sign (Fig. 7b). This state is analogous to the 1p state. Now suppose that the width of the right hand well is changed to a' , where $a' < a$ (Fig. 7c). It is well known that when this happens, the amplitude of the wave function increases in the smaller left hand well, rather than flowing into the larger right hand well (Fig. 7d). Thus, the pressure exerted by the particle in the smaller well will increase. Hence, the system has a natural stability.

We can also consider the more realistic model of the final stage of the fission process shown in Fig. 8a. We suppose that at this stage of the fission

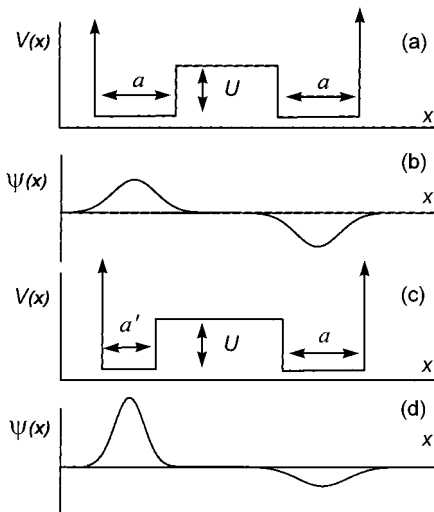


Fig. 7. The double well model discussed in the text. For the potential (a) the wave function (b) is such that the particle has an equal probability of being found in either well. When the left hand potential well is made narrower as in (c), the probability of finding the particle in the left hand well increases as shown in (d).

process, the original single bubble has been distorted into a volume consisting of two spheres of radius R_1 and R_2 that have a small overlap. We take the total energy of this system to be

$$E = E_{\text{el}} + 4\pi R_1^2 \alpha + 4\pi R_2^2 \alpha, \quad (10)$$

where E_{el} is the energy of the electron, and the correction to the surface area due to the small amount of overlap of the spheres has been neglected. For simplicity, we restrict attention to zero pressure. To calculate E_{el} , we write the wave function as

$$\psi = c_1 \psi_1 + c_2 \psi_2, \quad (11)$$

where c_1 and c_2 are amplitudes, and we have used as basis states 1s wave functions ψ_1 and ψ_2 inside each of the two spheres. The energies of the basis states are

$$E_1 = \frac{h^2}{8mR_1^2} \quad E_2 = \frac{h^2}{8mR_2^2} \quad (12)$$

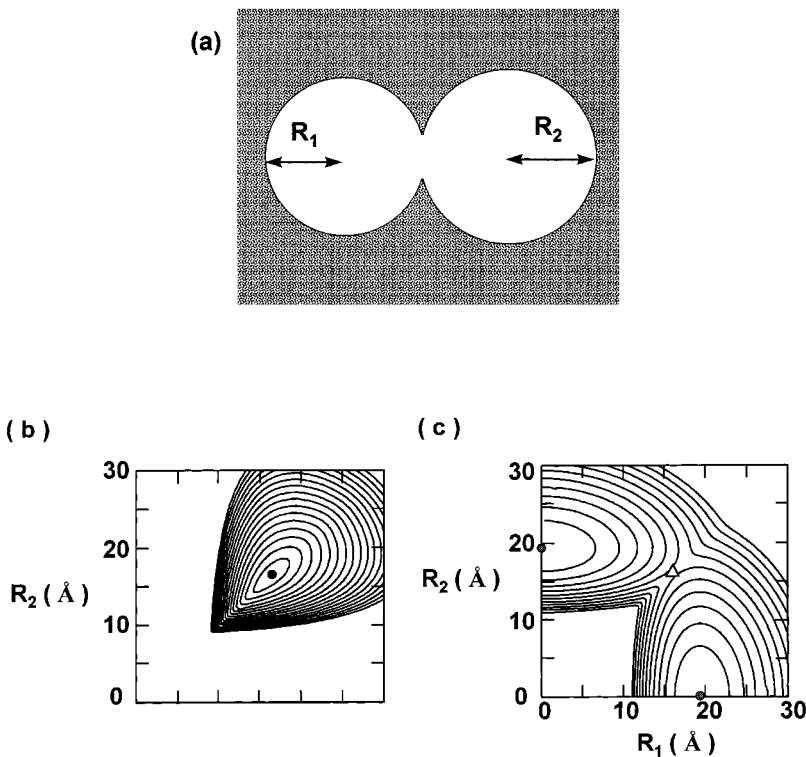


Fig. 8. (a) Geometry of the model used to study the stability of the fission process. (b) Contour plot of the energy as a function of the radii R_1 and R_2 when the electron is in the excited state. The solid circle shows the configuration of minimum energy. The contour closest to the minimum corresponds to an energy of 4.8×10^{-13} ergs. (c) Contour plot of the energy when the electron is in the ground state. The open triangle shows the location of a saddle point, and the two solid circles are minima. The contours closest to the minima correspond to an energy of 3.4×10^{-13} erg. The energy difference between adjacent contours is 0.2×10^{-13} erg.

Let the rate for quantum tunneling of the electron through the neck between the spheres be Γ . This will be a sensitive function of the degree of overlap of the spheres. The electron energy is given by

$$E_{\text{el}} = \frac{E_1 + E_2 \pm [(E_1 - E_2)^2 + 4h^2\Gamma^2]^{1/2}}{2} \quad (13)$$

The + sign gives the energy of the excited state. This will be the energy that the $1p$ state will have after the bubble has reached the shape shown in Fig. 8a. The total energy E from Eq. (10) is plotted as a function of R_1

and R_2 in Fig. 8b. This plot is for a fixed value of Γ chosen to be 10^{13} sec^{-1} , which corresponds to $\hbar\Gamma = 0.0066 \text{ eV}$. It can be seen from the figure that there is a single stable minimum with $R_1 = R_2 = 16.2 \text{ \AA}$. A different choice for the value of Γ changes the form of the contour lines in Fig. 8b, but the stable minimum with $R_1 = R_2$ remains. Thus, we conclude that even when the bubble is close to splitting into two parts, the electron divides equally between the two spheres.

The electron energy in the ground state is obtained by taking the negative sign in Eq. (13). The total energy is plotted in Fig. 8c. There is now a saddle point at $R_1 = R_2 = 16.2 \text{ \AA}$, and minima at $R_1 = 0, R_2 = 19.4 \text{ \AA}$, and $R_1 = 19.4 \text{ \AA}, R_2 = 0$. Thus, as expected, when the electron is in its ground state, the lowest energy configuration is with the wave function confined in a single bubble.

We have not considered the stability of other excited states.

E. Properties of Bubbles Containing Fractional Electrons

We will call the bubbles that contain a fraction of the wave function of an electron, electrino bubbles, and will denote a bubble in which the integral of $|\psi|^2 = f$ by e^f . If the penetration of the wave function is neglected, the radius of a $1s e^{1/2}$ bubble will be smaller than the radius of an ordinary electron bubble by a factor of $2^{1/4}$. Based on the discussion at the end of Sec. II (see the questions 1–3 that were raised at that point), it is not clear that quantum mechanics, as currently developed, provides definite predictions regarding the properties of these objects. For example:

(1) At what wavelengths will such bubbles absorb light? One approach is the following. The wave function inside one of the electrino bubbles is a $1s$ wave function normalized so that the integral of ψ^2 over the bubble is $\frac{1}{2}$. We apply an oscillating electric field to this bubble and find the frequencies at which absorption of energy takes place. Since the time-dependent Schrödinger equation is linear in ψ , these frequencies are unaffected by the normalization of the wave function, i.e., optical absorption occurs at the same photon energies as for an ordinary electron bubble of the same radius. Figure 9 shows the photon energy for the $1s \rightarrow 1p$ transition. The results in Fig. 9 are based on the same model approximations that were used for Fig. 3, i.e., the surface tension was assumed to have the value $0.341 \text{ erg cm}^{-2}$ independent of pressure, the polarization energy was neglected, and the Wigner–Seitz approximation was used for the height V_0 of the energy barrier. Based on this model, the bubble radius for zero pressure is found to be 14.8 \AA .

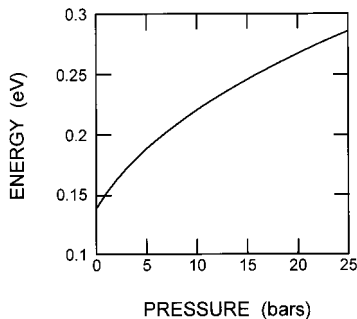


Fig. 9. Energy of the $1s \rightarrow 1p$ transition for an $e^{1/2}$ electrino bubble as a function of pressure.

Alternatively, one could make the argument that if light is to be absorbed in the bubble, the electron must be there. Hence, the bubble will have the normal size, and will absorb light at the same energies as does the normal bubble.

(2) We can ask about the results of other experiments that effectively measure the size of the bubble. It might be possible to measure the effective mass of the bubble, as has been done for normal bubbles.¹⁹ The mobility of a bubble at finite temperatures is proportional to the charge and varies inversely as the drag force F_{drag} on the bubble that arises from the interaction of the bubble with phonons and rotons. This drag force depends on the size of the bubble. To predict the results of these two experiments, it is necessary to know how to treat the charge on the bubble, i.e., does the bubble act as though it has charge $\frac{1}{2}e$, or does it behave as though it has a full charge? It is not clear that quantum mechanics gives a definite answer to this question, and the answer may depend on the particular experiment. Consider, for example, an experiment to measure the mobility of $e^{1/2}$ bubbles that uses a cell with travel distance w , and an applied electric field E . Suppose that an electron is injected from the cathode at one end of the cell, and is then optically excited so that two $e^{1/2}$ bubbles are produced. Let us suppose that the anode of the cell together with the electronics connected to it acts as a "measurement device" in the quantum mechanical sense. If the measurement device indicates that an electron has arrived, the work that has been done by the electric field must be eEw (E is the electric field, w is the distance across the cell). This should equal the total energy dissipated by the viscous drag force acting on the bubble (or bubbles) that have crossed the cell. The drag force F_{drag} acting on a bubble moving at small velocity equals γv , where γ is a coefficient that

depends on the size of the bubble. It could be argued that in this experiment two $e^{1/2}$ bubbles move through the liquid from the cathode to the anode, where the measurement device “finds” an electron in one of them. According to this view the dissipation is $eEw = 2\gamma_{1/2}vw$, where $\gamma_{1/2}$ is the drag coefficient for an $e^{1/2}$ bubble. Thus, the mobility would be $\mu = v/E = e/2\gamma_{1/2}$. Hence, the conclusion is that the mobility of the $e^{1/2}$ bubble should be calculated using one half of the full charge of one electron together with the drag force on the bubble of reduced size. However, this argument supposes that there is energy dissipation in the liquid along the path of the $e^{1/2}$ bubble in which an electron is *not* found. If we take the viewpoint that this dissipation does not occur, we would instead be lead to the conclusion that the mobility should be $\mu = e/\gamma_{1/2}$, i.e., the $e^{1/2}$ bubble acts as though it has the full charge.

(3) Assuming that electron bubbles in excited states do divide into two or more pieces, we can ask what will be the interaction between the pieces. Let us suppose that the correct procedure is as follows. If the electron is inside one of the bubbles at position \vec{r} there will be an electric field $\vec{E}(\vec{r}, \vec{r}')$ at the point \vec{r}' . Hence the energy associated with the polarization of the helium will be

$$-\frac{1}{2}\alpha_{\text{He}} \int |\vec{E}(\vec{r}, \vec{r}')|^2 d^3\vec{r}', \quad (14)$$

where α_{He} is the polarizability of liquid helium per unit volume, and the integral is over the volume occupied by liquid. This result is correct to first order in α_{He} , and it has been assumed that the density of the liquid is unaffected by the electric field. The polarization energy as given by Eq. (14) is then averaged over all possible positions of the electron, giving the result

$$E_{\text{polzn}} = -\frac{1}{2}\alpha_{\text{He}} \iint |\psi(\vec{r})|^2 |\vec{E}(\vec{r}, \vec{r}')|^2 d^3\vec{r} d^3\vec{r}'. \quad (15)$$

As the bubbles move further away from each other, there is a greater volume of helium in the region of strong electric field and hence the polarization energy decreases, i.e., becomes more negative. Thus, there is a weak repulsive interaction between the electrino bubbles. The potential as a function of the separation as calculated from Eq. (15) is shown in Fig. 10.

Of course, one could also consider other contributions to the interaction energy coming from, for example, exchange of phonons or the long range van der Waals interaction between helium atoms. These appear to be smaller effects, but we have not investigated them in detail.

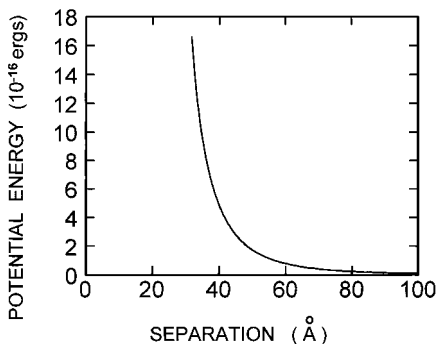


Fig. 10. Energy of interaction between two $e^{1/2}$ electrino bubbles as a function of the distance between the centers of the bubbles. The interaction energy arises from the polarization of the liquid helium, as described in the text.

IV. EVIDENCE FOR FRACTIONAL ELECTRONS

Based on the above theoretical work, we expect that electrino bubbles will be formed when ordinary electron bubbles are excited by light. We have examined this process in detail for the $1s \rightarrow 1p$ transition only, but it seems likely that electrino bubbles are produced after other bound-bound transitions, such as the $1s \rightarrow 2p$. It also appears likely that electrino bubbles will be produced after an electron is ejected from a bubble into an unbound state. At the present time, we do not know how to calculate the probability of production of electrino bubbles after a bound-unbound optical transition, or what fraction electrinos are produced. There is also the possibility that when the optical illumination contains a number of different wavelengths, electrino bubbles that have been produced as a result of a first fission process can undergo further division. Finally, we have to consider the possibility that electrino bubbles can be formed directly when an energetic electron enters helium and comes to rest. Again, we do not know how to calculate the probability with which electrino bubbles are produced by this mechanism. Through the combination of these different mechanisms, it appears likely that bubbles containing a substantial number of different fractions of an electron can be produced. We have looked at the existing literature for evidence of electrino bubbles. We have found that there are, in fact, a number of experimental observations that can be interpreted as evidence for the existence of these bubbles. It is significant that, as discussed below, these experimental observations have hitherto defied explanation.

A. Photoconductivity Experiments

The theory that we have presented predicts that if light is absorbed by a bubble with the electron in the ground state, the bubble will split into two parts. The electrino bubbles will be smaller than the original bubble. The mobility of a bubble in liquid helium depends on its size (see detailed discussion below). Thus, our theory predicts that there should be a photoconductivity effect, i.e., if the liquid is illuminated with light of the correct wavelength, the ionic mobility should be modified. This modification of the mobility should occur for light wavelengths that can excite the $1s \rightarrow 1p$ and $1s \rightarrow 2p$ transitions. It is also possible that electrino bubbles can be produced by light of wavelength sufficiently short to excite the electron out of the bubble and into a free state.

A second prediction of our theory is that this photoconductivity effect is likely to disappear above some temperature. As the temperature is increased the number of phonons and rotons in the liquid increases, and the motion of the wall of the bubble will be damped. Above a critical temperature T_c , the damping will become sufficiently large that fission will no longer occur (see previous discussion concerning Fig. 6). It is hard to perform a quantitative calculation of T_c , but we note the following points. Gross and Tung-Li²⁰ have calculated the frequencies of the normal modes of an electron bubble. Using their results, it is straightforward to show that for helium above the lambda point, the $l=0$ and $l=2$ oscillations of a bubble are heavily damped, i.e., most of the vibrational energy is lost in less than half a cycle. This indicates that T_c must have a value below T_λ . As the temperature is reduced below T_λ , the mean free path of rotons and phonons quickly becomes larger than the bubble diameter, and so it is no longer permissible to use the two-fluid model to calculate the damping of the bubble wall. The damping of the motion of the bubble wall could perhaps be calculated by using the measured mobility of negative ions in superfluid helium to estimate the drag on the bubble wall due to phonon-roton interactions. It would then be necessary to determine over what range of temperature this drag force is large enough to prevent fission.

Experiments to study the effect of light on ionic mobility have been conducted by Northby and Sanders,^{21, 22} Zipfel and Sanders,^{12, 13} and Grimes and Adams.^{10, 11} They observed an increase in ionic mobility under illumination, but recognized that the origin of the effect was unclear. It appears that the electrino bubble provides a natural explanation for the majority of the results that they obtained. We now summarize these results.

In the Northby and Sanders (NS) experiment,^{21, 22} ions were introduced into the liquid from a radioactive source, and had to pass through two grids in order to reach the detector. The voltages on the grids were

varied in time in a way such that normal negative ions could not reach the detector. It was found that when the liquid was illuminated, a small ion current reached the detector. The goal of the experiment was to detect the photo-ejection of electrons from bubbles. It was assumed that if an electron was ejected, it would have a very high mobility and therefore be able to reach the detector. NS measured the photo-induced current with light of photon energy E_ν from 0.7 to about 3 eV. They found that the photo-induced current had a peak when the photon energy was $E_1 = 1.21$ eV. They then made a calculation of the probability of photo-ejection, in which the bubble radius was adjusted so that a strong peak in the calculated photo-ejection spectrum occurred at the energy E_1 . The bubble radius they obtained in this way was 21.2 Å.

An electron that is ejected from a bubble into helium will lose its kinetic energy very quickly, and will then form a new bubble. As far as we can see, the time scale for this to happen should be of the same order of magnitude as the time scale for bubble shape oscillations, i.e., of the order of 10^{-10} to 10^{-11} secs. Thus, we believe that the ejection of the electron from the bubble is not likely to decrease significantly the transit time of the electron across the experimental cell.

In the work of Zipfel and Sanders (ZS), similar measurements to those of NS were made as a function of pressure up to 16 bars.^{12, 13} The photo-conductivity peak detected by NS was found to shift to higher photon energies as the pressure increased. In addition, a second peak was found at a lower photon energy E_2 . At zero pressure, this peak was at approximately 0.5 eV. NS assumed that the peak at E_2 was a second peak in the photo-ejection spectrum. They performed further calculations of the photo-ejection spectrum, and showed that by choosing a smaller radius for the bubble (around 15 Å for $P=0$), a spectrum could be obtained that contained peaks at both E_1 and at E_2 .

Miyakawa and Dexter²³ performed calculations of the optical absorption of an electron bubble, and concluded that the peak at E_2 seen by ZS corresponded to the transition $1s \rightarrow 2p$, and that the peak at E_1 seen by NS and also by ZS corresponds to ejection of an electron from the bubble. Miyakawa and Dexter also calculated the photon energy required for the $1s \rightarrow 1p$ transition. This transition was detected by Grimes and Adams (GS),¹⁰ again through a measurement of photoconductivity. Shortly after this, the transition was seen by Parshin and Pereversev²⁴ and by Grimes and Adams¹¹ in direct measurements of optical absorption.

Although these experiments have established the electron transitions that are responsible for each peak in the photoconductivity, it was difficult to understand why there should be a change in conductivity when light was absorbed. Miyakawa and Dexter²³ proposed that when light was absorbed

by the bubble, it would be set in vibration, and the vibrational energy would quickly be converted into heat. If the bubble were attached to a vortex, this heating could enable it to escape, and so there would be an increase in current. In the Grimes and Adams experiment, ions were introduced by field emission from sharp tips. Near to the tips, the electric field was very large, and so it reasonable to assume that a large number of vortices were present. However, it seems unlikely that this mechanism can explain the data of NS and ZS. In their experiments, the illumination was applied far away from the ion source. It appears that the voltages that were applied to the grids were too small for vortex nucleation by the ions moving through the liquid at the temperature of the experiment (1.3 K). In addition, we note that in the ZS experiment measurements were made up to a pressure of 16 bars. It is known²⁵ that above pressures of about 10 bars, when a strong electric field is applied, the normal negative ion loses energy by roton production and does not produce vortices.

Our proposal is that the photo-conductivity effect arises from the creation of electrino bubbles by the light. Our explanation does not rely on the assumption that vortices are present.

In the experiments of NS, ZS and GA it was noted that the photo-conductivity effect was absent above a critical temperature. This temperature was approximately 1.7 K at zero pressure, and decreased to 1.2 K at 20 bars. Grimes and Adams¹⁰ proposed that this effect occurred because at a critical temperature the probability that a vortex line will trap a negative ion becomes very small. We propose instead that the photoconductivity signal disappears because of the damping of the bubble motion by the excitations in the liquid. As the pressure is increased, the roton energy gap goes down, and so the damping increases. Thus, it is to be expected that T_c decreases with increasing pressure.

B. Exotic Ions

In a paper published in 1969, Doake and Gribbon²⁶ detected negatively-charged ions that had a mobility substantially higher than the normal electron bubble negative ion. Measurements were made by a time-of-flight method. This ion, which has become known as the "fast ion," was next seen in another time-of-flight experiment by Ihas and Sanders (IS) in 1971.²⁷ They showed that the fast ion could be produced by an α or β source, or by an electrical discharge in the helium vapor above the liquid. In addition, they reported the existence of two additional negative carriers, referred to as "exotic ions," that had mobilities larger than the mobility μ_n of the normal negative ion, but less than the mobility μ_f of the fast ion. These exotic ions were detected only when there was an electrical discharge

above the liquid surface. In a paper the following year,²⁸ IS reported on further experiments in which 13 carriers with different mobilities were detected. Measurements could be made only in the temperature range 0.96 to 1.1 K, where the density of the helium vapor was such that an electrical discharge could be produced. The strength of the signal associated with each carrier depended in a complicated way on the magnitude of the voltage used to produce the discharge and on the location and geometry of the electrodes. Figure 11 shows the mobilities μ_2 , μ_4 , and μ_8 of the three exotic ions that gave the strongest signals, together with the mobility of the normal bubble and the fast ion.²⁹ The IS experiments are described in detail in the thesis of Ihas.³⁰ More recently, these ions have been studied by Eden and McClintock (EM).^{31, 32} They also detected as many as 13 ions with different mobilities. In their measurements, the mobility in large electric fields was studied, whereas IS investigated the mobility in low fields. EM showed that, like the normal ion, the exotic ions nucleate vortices when their velocity reaches a critical value v_c . This critical velocity was found to be larger for the exotic ions of higher mobility.

The ions studied by IS have mobilities that lie in a range up to about five times the mobility of the normal negative ion. If we assume that the mobility of the ion varies as the inverse square of its radius R (see discussion below), it follows that the 13 carriers must have radii between about

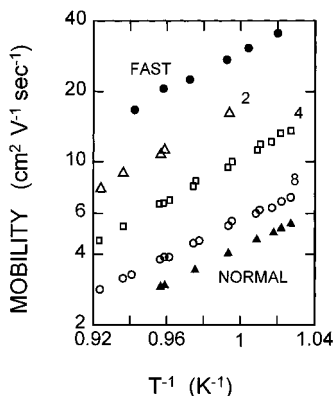


Fig. 11. Mobility of negative ions in superfluid helium plotted versus the inverse of the temperature. Solid triangles are for the normal electron bubble, open squares, circles and triangles are for three of the exotic ions, and solid circles are the fast ion. These data are taken from ref. 30.

9 and 18 Å. Donnelly and Roberts' theory of the critical velocity for vortex nucleation predicts that v_c should increase as the radius of the ion decreases.³³ The experiments of EM show that the critical velocity for vortex production is higher for the exotic ions of higher mobility, and are thus consistent with Donnelly and Roberts' prediction.

Both IS and EM put forward a number of proposals to explain the exotic ions, but considered all of these to be unsatisfactory. These proposals included the following: (1) A free electron, i.e., an electron that has not formed a bubble, will have a higher mobility than the normal negative ion. However, the mobility is expected to be two orders of magnitude higher, whereas the exotic ions have mobilities that are no more than a factor of five larger than the normal ion. In addition, as already mentioned, it is expected that a free electron will form a bubble state very quickly; (2) An electron bubble with the electron in an excited state should have a different mobility from the normal ion. However, as we have seen in Sec. IIIB, when these bubbles have reached an equilibrium shape they are larger than the 1s bubble, and so should have a lower mobility. In addition, the lifetime of the excited states¹⁵ is less than the time for the exotic ions to cross the mobility cell; (3) An electron bubble containing two electrons would have a different mobility from the normal ion. But calculations of the energy of this complex show that it has an energy substantially higher than the energy of two single electron bubbles, and therefore is unstable.³⁴ Also based on the theoretically-predicted size of the two electron bubble, it is expected that it will have a lower mobility than the normal ion; (4) The exotic ions might be negative helium ions (He^-). However, the lifetime of these ions in vacuo is short, and so it would be necessary to suppose that for some reason their decay takes place at a much slower rate when they are in the liquid. In addition, the lifetime of the He^- ion is greatly reduced by the application of a magnetic field. Ihas and Sanders found that the exotic ions could still be detected even in the presence of a field of 1.2 kG; (5) The exotic ions could be negatively charged impurities in the helium. In the IS and EM experiments the electrical discharge in the helium vapor could cause sputtering of atoms from the cell walls. Some of these atoms could be negatively charged. However, for an atom with a large electron affinity (e.g., 2 eV), the electron wave function will decrease rapidly with distance from the atom. When such an ion is in liquid helium, the bubble that will be produced will be very small.³⁵ Therefore to produce objects that have a size indicated by the mobility measurements, it is necessary to consider impurity atoms that have a very small electron affinity. We have performed calculations of the variation of the size of an impurity ion with the electron affinity.³⁶ We find that to get a bubble with a radius in the required range (i.e., with a radius greater than 9 Å) it is necessary for the

electron affinity to be less than about 0.2 eV. There are only a small number of elements that meet this requirement. These include iron that might well be sputtered from some part of the experimental cell, and nitrogen that is likely to be adsorbed on the cell walls. However, as far as we can see, it is not possible to explain the existence of 13 different exotic ions in this way. We note that negatively-charged impurities may well be the explanation of the fast ion.

It is significant that the exotic ions appear only when an electrical discharge takes place close to the free surface of the liquid. Under these conditions, the electrons that enter the liquid and form bubbles may absorb light emitted from the discharge. Thus, it is natural to consider the possibility that the exotic ions are bubbles containing fractional electrons. As mentioned at the beginning of this section, it appears that the fraction f of an electron confined in a bubble could take on a number of different values, and so this could conceivably explain the existence of ions with 13 different mobilities.

To associate a definite fraction f with each one of the ions seen by IS and EM, it is necessary to have a detailed theory of how the mobility m of a bubble varies with f . Unfortunately, it appears to be extremely hard to construct a quantitative theory for μ as a function of f . In the temperature range around 1 K, the ionic mobility of the normal electron bubble is primarily limited by roton scattering. If the roton-ion scattering cross-section is taken to have a constant value σ_{IR} and the recoil of the ion is neglected, the mobility is³⁷

$$\mu = \frac{3\pi^2 e}{\hbar k_0^4 \sigma_{\text{IR}}} \exp(\Delta/kT), \quad (16)$$

where e is the charge on the electron, k_0 is the wave number at the roton minimum (1.91 \AA^{-1}), and Δ is the roton energy gap. As a first guess, we can take the cross-section σ to be the geometrical cross-section πR^2 . This gives a mobility for the normal ion (using the theoretical value of $R = 19.4 \text{ \AA}$) of $2.9 \times 10^{-4} \exp(-\Delta/kT) \text{ cm}^2 \text{ V}^{-1} \text{ sec}^{-1}$. At 1 K this equals $1.7 \text{ cm}^2 \text{ V}^{-1} \text{ sec}^{-1}$ which is about 40% of the measured value for the normal ion. To develop a more accurate theory the following effects need to be included: (1) When a roton collides with a bubble, the bubble recoils due to its finite mass. The effect of recoil has been considered by Barrera and Baym,³⁸ and by Bowley.³⁹ Allowance for recoil modifies the magnitude of the mobility and also the temperature-dependence. (2) When a roton scatters from the bubble, it can be reflected as a normal or anomalous roton, i.e., a roton with group velocity opposed to its momentum. The probabilities of these two processes are unknown, and affect the result for

the mobility and the form of the correction for recoil just discussed.⁽³⁹⁾ (3) Finally, the relation $\sigma = \pi R^2$ between the total scattering cross-section σ and the bubble radius R , as used in the calculation of the bubble energy, is unlikely to be quantitatively correct.

Exotic ions that have mobilities close to the mobility of the normal ion must have a radius R close to the radius R_n of the normal ion. For these ions, it may be a reasonable approximation to estimate the mobility μ using

$$\frac{\mu}{\mu_n} = \frac{R_n^2}{R^2}. \quad (17)$$

From the data of IS, the value of μ/μ_n averaged over the data points for ion #8 is 1.31 (see Fig. 11). Now we compare these values with what might be expected for electrino bubbles. On the basis of the very simplest model of the electron bubble [see Eq. (4)], the radius $R_{1/2}$ at zero pressure for an $e^{1/2}$ bubble should be the radius R_n of the normal negative ion divided by a factor of $2^{1/4}$. Hence on this model, and assuming that the full charge should be used to determine the mobility, the mobility should be $1.41\mu_n$. This mobility is thus fairly close to the mobility of the exotic ion #8 as measured by Ihas and Sanders.⁴⁰ If we allow for the penetration of the wave function into the helium, the mobility calculated from Eq. (17) is $1.45\mu_n$. Inclusion of the polarization correction gives $1.38\mu_n$.⁴¹

Given the absence of a quantitative theory of the mobility, it is impossible to make a serious estimate of the size and value of f for the

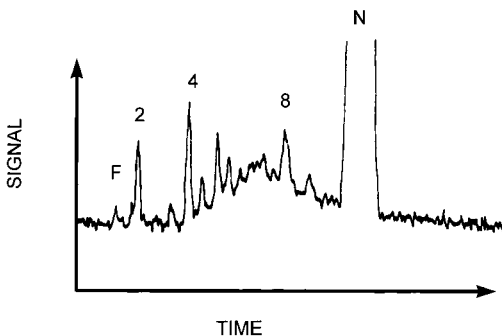


Fig. 12. Data trace taken from ref. 30 showing the detected ion signal as a function of time. F and N denote the fast and normal ion signals. 1, 2, and 3 are the peaks corresponding to the same exotic ions shown in Fig. 11. For a description of the experimental conditions, see ref. 30.

other exotic ions. We note, however, one interesting aspect of the IS data that apparently has not been noticed. We show in Fig. 12 one of the data traces taken from the thesis of Ihas.⁴² The pulses arising from the fast and normal ions, along with the pulses from the three exotic ions, are labeled as in Fig. 11. It can be seen that there is a broad background signal in addition to the sharp pulses. Two possible explanations of this come to mind. An electron entering the liquid could form a normal ion and then, after traveling some distance be converted by photo-excitation into an exotic ion. Since, the conversion could occur at different depths for different ions, a broad distribution of arrival times would result. A second interesting possibility is that there are processes that lead to electron bubbles in which f can have a continuous range of values.

V. SUMMARY AND OPEN QUESTIONS

We summarize the main points of this paper:

(1) We first discussed experiments which result in the wave function of a particle becoming confined within two separated regions of space. We argue that quantum mechanics does not make clear predictions for the results of measurements on systems with a wave function of this type.

(2) We then considered the behavior of an electron bubble that undergoes optical excitation. We show that, in the absence of damping of the liquid motion, the bubble will split into two smaller bubbles each containing a wave function ψ such that the integral of $|\psi|^2$ over the volume of the bubble gives $\frac{1}{2}$. The sum of the energy of the two $e^{1/2}$ bubbles is less than the energy that the single bubble has after optical excitation.

(3) We have calculated the photon energy required to excite these electrino bubbles to the $1p$ state, and the interaction energy between the two bubbles.

(4) Finally, we discussed the possibility that the electrino bubbles have already been produced in several experiments involving ions in superfluid helium. It has hitherto been impossible to explain the results of these experiments in a reasonable way. We showed that it may be possible to explain these experiments in terms of electrino bubbles. Of course, it is possible that not *all* of the effects observed in these experiments are to be attributed to electrino bubbles. We find that in order for the exotic ions to be electrino bubbles, it is necessary to assume that the bubbles act as though they have the full charge of an electron.

We want to emphasize that even if further experiments show that electrino bubbles are not involved in the experiments that we have discussed,

the theory we have given predicts the existence of these objects. We note that the calculations mentioned in (2) above rely on a number of well-tested principles borrowed from molecular physics. The time scale of the motion of the electron is much less than the time scale for motion of the bubble wall. Thus, the Franck–Condon principle should apply. The difference in time scales also means that as the bubble shape changes, the wave function of the electron will deform adiabatically (Born–Oppenheimer principle). The application of these principles, together with the use of Schrödinger’s equation for the calculation of the energy of the electron states, leads to the prediction that the electron will undergo fission. Given these considerations, we have to consider that it would be an interesting result if electrino bubbles were shown to *not* exist.

Finally, we note the following points:

(1) It should be possible to make detailed studies of the bubbles via optical techniques. For example, it should be possible to create $e^{1/2}$ bubbles by optical excitation of the $1p$ state of the normal negative ion, and then measure the mobility of these measured by means of a time-of-flight experiment. It would then be possible to determine if the measured mobility of this ion matches the mobility of one of the exotic ions already studied experimentally. It should also be possible to provide a second optical wavelength to cause a second fission and produce $e^{1/4}$ bubbles. The mobility of these could then be measured.

(2) In order for the electrino bubbles to be the explanation of the experiments on exotic ions, it is necessary to suppose that, as far as mobility experiments are concerned, the bubbles that reach the detector act as though they have the full charge of the electron. This needs further experimental study. Does this mean that some of the bubbles act as though they have one unit of negative charge and others act as though they have no charge? An experiment that probed the spatial distribution of the electrino bubbles in a helium cell could answer this question.

(3) One can ask what happens to these objects when they leave the liquid. For example, can the part of the wave function confined within an $e^{1/2}$ electrino bubble bind to an atom or ion on the cell wall? If this happens, what are the chemical properties of such an atom that has captured half of the wave function of an electron? Or does the arrival at the cell wall amount to a quantum measurement process, so that the other part of the wave function (which is in another bubble some distance away) collapses along with the bubble containing it? If this happens, is there a measurable energy release into the liquid?

(4) Is our calculation of the energy of interaction between two electrino bubbles produced by the splitting of one electron correct? It should

be possible to test this result experimentally.? Is there any interaction between a pair of electrino bubbles, other than the polarization interaction that we have considered? Is there any limit to the separation between the bubbles? And, it is natural to ask whether it is possible to separate the liquid helium into two volumes, each containing one of the pair of electrino bubbles.

(5) Finally, it would be very interesting to consider other situations in which the fission of an electron or other elementary particle might occur. Fission of bubbles after optical excitation between two bound states should not occur in liquid helium-4 above the lambda point or in the normal phase of helium-3 because the viscosity of these liquids damps the motion of the bubble wall. It is also interesting to look for other physical situations in which fission occurs "naturally," i.e., as a result of a spontaneous mechanism analogous to the process that takes place with a bubble in helium absorbs a photon, and that does not involve any external interaction other than the absorbed photon. If such a situation existed in the early universe, for example, it might provide a mechanism for the production of exotic particles with unusual charge properties that might be hard to detect by conventional means. It may also be possible to design and construct a solid state device that can be used to divide electrons.

ACKNOWLEDGMENTS

I thank S. Balibar and G. M. Seidel for many helpful discussions and encouragement. I would also like to thank R. M. Bowley, M. W. Cole, L. N. Cooper, J. A. Northby, A. V. Nurmikko, and C. Tan for help on a number of topics that came up while writing this paper, and H. H. Wickman for support at a critical stage of this research. This work was supported in part by the National Science Foundation through grants DMR 97-03529 and INT-9314295.

REFERENCES

1. A. Einstein, B. Podolsky, and N. Rosen, *Phys. Rev.* **47**, 777 (1935).
2. N. Bohr, *Phys. Rev.* **48**, 696 (1935). See also, N. Bohr, in *Albert Einstein: Philosopher-Scientist*, P. A. Schilpp (ed.), Library of Living Philosophers, Evanston (1949), p. 200. For a discussion of the arguments put forward by Einstein, Podolsky and Rosen, and by Bohr, see D. Bohm, *Quantum Theory*, Prentice-Hall, New York (1951).
3. For a discussion, see A. J. Leggett, *The Problems of Physics*, Oxford, Oxford (1987).
4. The properties of ions in helium have been reviewed by A. L. Fetter, in *The Physics of Liquid and Solid Helium*, K. H. Benneman and J. B. Ketterson (eds.), Wiley, New York (1976), Chap. 3.
5. W. T. Sommer, *Phys. Rev. Lett.* **12**, 271 (1964).

6. L. B. Lurio, T. A. Rabedeau, P. S. Pershan, I. F. Silvera, M. Deutsch, S. D. Kosowsky, and B. M. Ocko, *Phys. Rev. B* **48**, 9644 (1993). This width is the distance over which the density changes from 10 to 90% of its bulk value.
7. J. Classen, C.-K. Su, M. Mohazzab, and H. J. Maris, *Phys. Rev.* **57**, 3000 (1998).
8. In recent unpublished work with D. Konstantinov, we have shown that the standard expression for the helium polarization contribution to the energy (as given, for example, in Ref. 4) is wrong. A corrected result will be published shortly. To calculate the polarization energy it is essential to make allowance for the quantum fluctuations in position of the electron inside the bubble.
9. For example, the theory of D. Amit and E. P. Gross (*Phys. Rev.* **145**, 130 (1966)) predicts that the surface tension increases by almost a factor of 2 when the pressure is varied from zero to 25 bars.
10. C. C. Grimes and G. Adams, *Phys. Rev. B* **41**, 6366 (1990). Grimes and Adams take the value of V_0 at zero pressure to be 1.02 eV.
11. C. C. Grimes and G. Adams, *Phys. Rev. B* **45**, 2305 (1992).
12. C. L. Zipfel, Ph.D. thesis, University of Michigan (1969), unpublished.
13. C. L. Zipfel and T. M. Sanders, in *Proceedings of the 11th International Conference on Low Temperature Physics*, J. F. Allen, D. M. Finlayson, and D. M. McCall (eds.), St. Andrews University, St. Andrews, Scotland (1969), p. 296.
14. B. DuVall and V. Celli, *Phys. Lett. A* **26**, 524 (1968), and *Phys. Rev.* **180**, 276 (1969).
15. W. B. Fowler and D. L. Dexter, *Phys. Rev.* **176**, 337 (1968).
16. See, for example, R. Schinke, *Photodissociation Dynamics*, Cambridge (1993).
17. Note that the bubble radius is now 19.4 Å instead of 17.9 Å because the wave function is required to go to zero at the bubble surface.
18. Of course, the calculations of the energy are not really accurate to four significant figures. It is the variation of the energy with a_0 and a_2 that is important for the fission process.
19. T. Ellis, P. V. E. McClintock, and R. M. Bowley, *J. Phys. C* **16**, L485 (1983).
20. E. P. Gross and H. Tung-Li, *Phys. Rev.* **170**, 190 (1968).
21. J. A. Northby, Ph.D. thesis, University of Minnesota (1966), unpublished.
22. J. A. Northby and T. M. Sanders, *Phys. Rev. Lett.* **18**, 1184 (1967).
23. T. Miyakawa and D. L. Dexter, *Phys. Rev. A* **1**, 513 (1970).
24. A. Y. Parshin and S. V. Pereverzev, *JETP Lett.* **52**, 282 (1990) and *JETP* **74**, 68 (1992).
25. See, for example, P. V. E. McClintock, *Z. Phys. B* **98**, 429 (1995).
26. C. S. M. Doake and P. W. F. Gribbon, *Phys. Lett. A* **30**, 251 (1969).
27. G. G. Ihas and T. M. Sanders, *Phys. Rev. Lett.* **27**, 383 (1971).
28. G. G. Ihas and T. M. Sanders, in *Proceedings of the 13th International Conference on Low Temperature Physics*, K. D. Timmerhaus, W. J. O'Sullivan, and E. F. Hammel (eds.), Plenum, New York (1972), Vol. 1, p. 477.
29. Our Fig. 11 uses the data and numbering scheme of Fig. 18 of Ref. 30. In Ref. 28 the ions that we have numbered as 2, 4, 8 are numbered 2, 6, and 11.
30. G. G. Ihas, Ph.D. thesis, University of Michigan (1971).
31. V. L. Eden and P. V. E. McClintock, *Phys. Lett. A* **102**, 197 (1984).
32. V. L. Eden, M. Phil. thesis, University of Lancaster (1986).
33. R. J. Donnelly and P. H. Roberts, *Phil. Trans. Roy. Soc. A* **271**, 41 (1971). See, in particular, Table 10 of this paper. The fact that the critical velocity could be used to estimate the size of the exotic ions has been pointed out by C. D. H. Williams, P. C. Hendry, and P. V. E. McClintock, *Phys. Rev. Lett.* **60**, 865 (1988). For more recent theory, see C. M. Muirhead, W. F. Vinen, and R. J. Donnelly, *Phil. Trans. Roy. Soc. A* **311**, 433 (1984).
34. D. L. Dexter and W. B. Fowler, *Phys. Rev.* **183**, 307 (1969). For an attempt to understand the exotic ions in terms of multielectron bubbles, see T. M. Sanders and G. G. Ihas, *Phys. Rev. Lett.* **59**, 1722 (1987).
35. In fact, if the binding is too large, the ion will form a snowball rather than a bubble.
36. Unpublished work. We thank Milton Cole for helpful discussions on this topic.
37. K. W. Schwarz and R. W. Stark, *Phys. Rev. Lett.* **22**, 1278 (1969).
38. R. Barrera and G. Baym, *Phys. Rev. A* **6**, 1558 (1972).

39. R. M. Bowley, *J. Phys. C* **4**, 1645 (1971).
40. The results of IS show that there is one exotic ion (#9) that has a mobility that lies between the mobility of the exotic ion #8 and the normal ion. If exotic ion #8 corresponds to $f = \frac{1}{2}$, ion #9 would have to have f greater than $\frac{1}{2}$. In order for f to be greater than $\frac{1}{2}$, it would be necessary for a normal electron bubble to split into two unequal parts. This seems unlikely, and so perhaps our assignment of $f = \frac{1}{2}$ to ion #8 is incorrect.
41. Here we have used what we believe to be the correct formula for the polarization energy. See Ref. 8.
42. This data trace is part of Fig. 15 of the thesis, and also appears in Ref. 28 with different numbering.